Resource Balance Analysis of Saccharomyces Cerevisiae

Eric Nazarenus

A thesis presented for the degree of

Bachelor of Science

Computational Cell Biology

Heinrich Heine University Düsseldorf

Germany

10 April 2023

Acknowledgments

I would like to express my gratitude to Prof. Dr. Martin Lercher for allowing me to work on this topic. I would also like to thank Prof. Dr. Oliver Ebenhöh for quickly agreeing to be the second assessor of this thesis. Furthermore, I would like to thank Peter Schubert for his extensive support and patience in our weekly meetings, helping me to find a topic for the thesis and guiding me throughout the whole process.

Finally, I thank Juliette Marie Bies for proofreading the thesis.

Abstract

Resource Balance Analysis (RBA) is a constraint-based modeling method used to investigate models of living cells based on the assumption that cells use their resources in an economically sensible way. Different RBA models have been made for prokaryotes such as *Escherichia coli*, *Bacillus subtilis* and *Ralstonia eutropha* with good predictive results. However, to our knowledge there have not been RBA models for eukaryotes such as *Saccharomyces cerevisiae* yet, as it was not clear in how far the RBA method can be applicable for eukaryotes.

In this study we create an RBA model for *Saccharomyces cerevisiae* and compare the results of various simulations against the results of other modelling methods. We show that the RBA modelling method can produce good results even for eukaryotes, specifically in terms of growth rates and certain metabolic phenomena. Finally, we discuss the limitations of our model and give ideas on how to further refine it.

Content

1 Introduction

One of the key goals of systems biology is the development of accurate metabolic models.
For the past 30 years constraint-based modelling has been a widely used modelling approach that aims to solve this goal by systematizing biochemical, genetic, and genomic knowledge into a mathematical framework that enables the calculation of metabolic fluxes from reactions' stoichiometry and intracellular metabolites' mass balances (Bordbar et al., 2014).
Over the course of these decades, multiple constraint-based genome-scale metabolic network reconstructions have been made, commonly referred to as GEMs (genome-scale metabolic models).
A prominent way to study these metabolic networks is called Flux Balance Analysis (FBA) which calculates the flow of metabolites through the network, thereby making it possible to simulate the growth rate of an organism or predict the rate of production of a biotechnologically important metabolite (Orth et al., 2010).
Achieving accurate simulation results is a goal for systems biology as it enables researchers to gain a better understanding of complex biological systems and predict their behavior under different conditions, potentially leading them to design experiments more efficiently and thus streamlining research in different areas.
FBA typically couples the uptake rate of the growth-inducing substrate (commonly the carbon source) linearly to the predicted growth, assuming that to be the main limitation of metabolite production, which results in no upper limit for growth predictions. This oversimplification can lead to inaccurate simulation results when compared to experimental data and often causes key phenotypic behaviors and phenomena to be missing from the model (Sánchez et al., 2017). In the case of *Saccharomyces cerevisiae*, an example for the key phenomena that FBA completely fails to portray would be the onset of overflow-metabolism at high glucose concentrations, known as the Crabtree Effect (De Deken, 1966).
Therefore, there has been interest in developing improved modelling methods that can integrate more complex information such as enzyme limitations or cell densities into a GEM to possibly improve the simulation accuracy.
Resource Balance Analysis (RBA) is a modelling method that includes many details, such as the amino acid composition of proteins, transport processes within a cell, and the composition and efficiency of molecular machines like enzymes or ribosomes (Goelzer & Fromion, 2017). In contrast to FBA, RBA assumes that the key element limiting growth rate is the resource allocation of macromolecules between all cellular processes (Coppens et al., 2023). Importantly, RBA models take enzyme limitations into account, coupling possible metabolic

fluxes to the corresponding enzyme requirements, which has been shown to lead to improved simulation results when compared to FBA, as seen in the enzyme constraint yeast model ecYeast7 that was created using the GECKO framework (Sánchez et al., 2017).

In this study we will construct an RBA model based on a GEM of the organism *Saccharomyces cerevisiae*. *S. cerevisiae*, also commonly known as baker's yeast is a unicellular, eukaryotic microorganism that is used as the eukaryotic model organism and due to its rapid growth rate and simple genetics, it has become one of the most well-understood and extensively studied organisms in molecular and cell biology (Botstein et al., 1997).

It is the aim of this study to create an RBA model for *S. cerevisiae* and investigate to what extent this RBA approach can lead to more accurate simulation results for the organism *S. cerevisiae* than simple Flux Balance Analysis and see how it compares to other approaches that include enzyme limitations into genome-scale models.

To address this question, we use some of the existing frameworks to create an RBA model, refine it by adjusting certain constraints and incorporating relevant experimental datasets and compare the results from the RBA simulations of different cellular behaviors to the corresponding results of the other methods and the experimentally observed results.

Additionally, we will investigate how far our model is able to portray certain key phenotypic behaviors that would not manifest in typical FBA simulations.

Finally, we will discuss the results our research has produced, the limitations of our method, and give an outlook on how to possibly refine and evolve our work further.

2 Preliminaries

In this section we will briefly give some background information and describe concepts to ensure that the reader is provided with all the necessary information to completely understand the sections that follow.

2.1 Linear Programming

Linear programming is a method for solving optimization problems that involve linear constraints and a linear objective function. Mathematically, a linear program in standard form is defined as follows (Bertsimas & Tsitsiklis, 1997):

$$max\ c^T x \quad (1)$$

$$subject\ to\ Ax \leq b \quad (2)$$

$$and \quad x \geq 0 \quad (3)$$

Where the objective function (1) is subject to the linear constraints (2). The goal of the linear program is to find the optimal solution for the objective function within the set of all possible solutions that satisfy the constraints. The LP solves for *x*, while *c* is a vector of coefficients representing the objective function, *A* is a matrix of coefficients representing the constraints and *b* is a vector of constants. Solving linear programs can be done computationally with multiple open-source or commercial solvers like GLPK (GLPK - GNU Project, n.d.) or CPLEX (Ilog CPLEX 8.0, 2002).

2.2 Flux Balance Analysis

Flux Balance Analysis (FBA) uses linear optimization to determine the steady-state reaction flux distribution in a metabolic network by maximizing an objective function, such as ATP production or growth rate (Raman et al., 2009). The linear optimization problem can be represented as follows:

$$max\ c^T v$$

$$subject\ to\ Sv = 0$$

$$and\ l_b \leq v \leq u_b$$

Where **S** represents a known stoichiometric matrix of coefficients, with rows representing metabolites and columns representing fluxes. The vector *v* represents all fluxes of the metabolic network and l_b and u_b represent the upper and lower bounds defined by the user for different fluxes, usually used for exchange reactions to define the medium.

2.3 GECKO and ecYeast

GECKO is a recently developed modelling method that extends GEMs by representing enzymes as entities with limited capacities in their corresponding reactions by expanding the stoichiometric matrix with additional columns for enzyme concentrations and additional rows to couple reaction fluxes to required enzyme concentration (Sánchez et al., 2017).

Additionally, the total amount of enzymes is limited by a density constraint and reactions that can be catalyzed by different isoenzymes are multiplied in order to have each reaction catalyzed by one specific enzyme.

Utilizing this approach Sánchez et al. have expanded the different versions of the Yeast Metabolic Network Reconstruction Yeast7 (Aung et al., 2013) and Yeast8 (Lu et al., 2019) GEMs and derived the respective enzyme constraint versions ecYeast7 and ecYeast8.

Through integration of the enzyme constraints ecYeast7 and ecYeast8 have both shown great promise in their predictive power across many different media compared to the default GEMs (Figure 1).

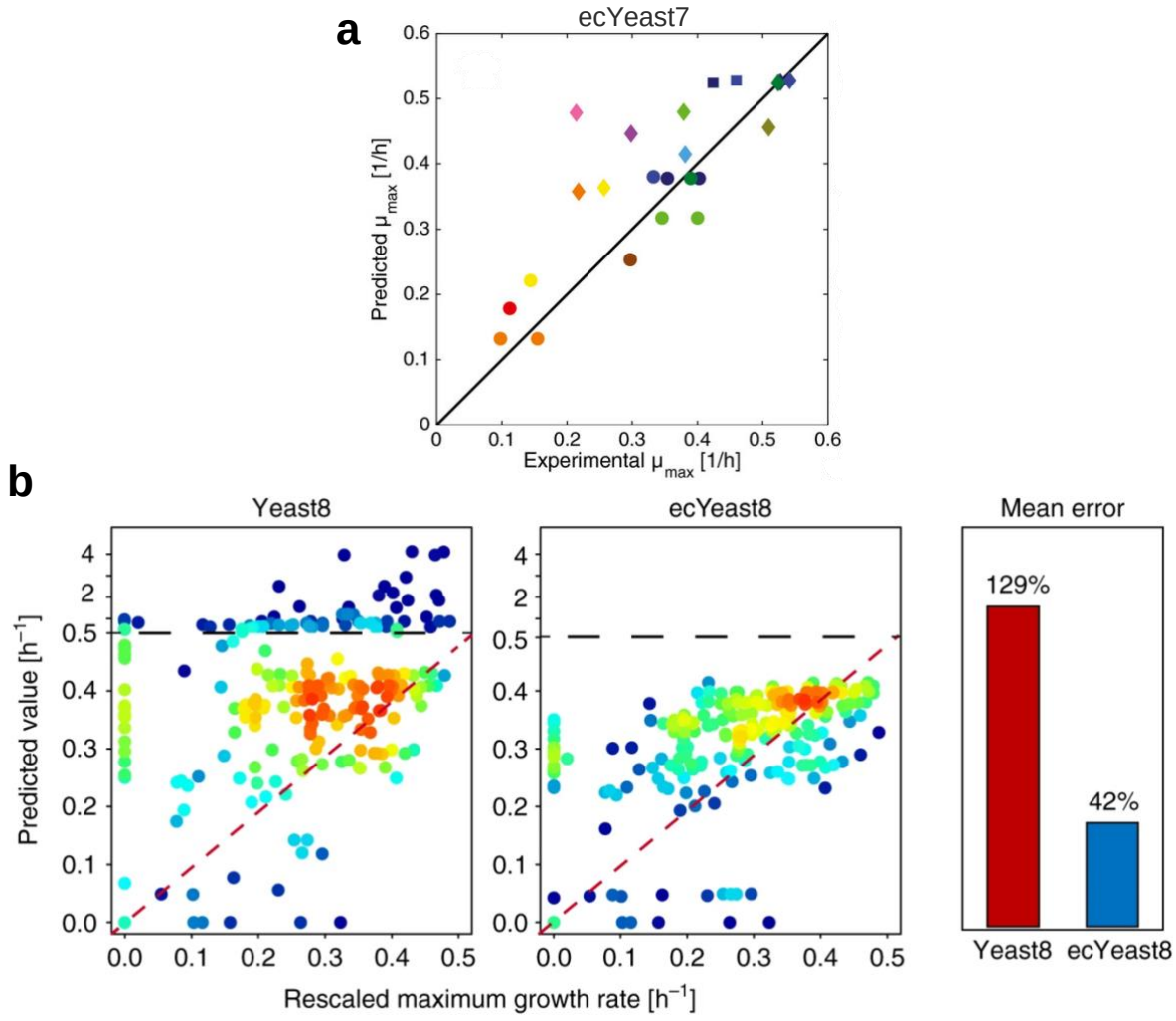

Figure 1: **Enzyme Constraints improving simulation results in *S. cerevisiae.* (a)** Prediction of maximum specific growth rates under 12 different carbon sources and three different media using ecYeast7. EcYeast7 shows an average relative error of 8%. Adapted from "Improving the phenotype predictions of a yeast genome-scale metabolic model by incorporating enzymatic constraints" by *Sánchez et al. (2017), Nature. Copyright by Creative Commons Attribution 4.0 International License* **(b)** Prediction of maximum specific growth rates under different combinations of carbon and nitrogen sources using Yeast8 and ecYeast8. Taken from "A consensus S.cerevisae metabolic model Yeast8 and its ecosystem for comprehensively probing cellular metabolism" by *Lu et al. (2019), Nature. Copyright by Creative Commons Attribution 4.0 International License.*

2.4 Resource Balance Analysis

Resource Balance Analysis (RBA) formulates a linear programming problem to calculate the highest feasible growth rate for a given RBA model. Originally RBA has been developed for the modelling of prokaryotic cells but in a recent paper Goelzer and Fromion (2019) investigate whether the RBA framework in theory could work for the modelling of eukaryotic cells as well. They make the case for a few more constraints that take the different cell organelles into account and ultimately concluded, that the original RBA optimization can be used for eukaryotic modelling as the linear optimization problems would be very similar and only a few changes mainly regarding the density constraints would have to be made.

The original optimization problem is as follows, taken from *RBA for eukaryotic cells: foundations and theoretical developments* (Goelzer & Fromion, 2019):

A cell is composed of different cellular entities:

(i) N_y molecular machines, that can be subdivided in N_m enzymes and transporters involves in the metabolic network (i.e. enzymes, transporters) $\mathbb{E} \triangleq (\mathbb{E}_1,\ldots,\mathbb{E}_{Nm})$ at the concentrations $\mathbb{E} \triangleq (E_1,\ldots, E_{Nm})^T$ and with the fluxes $v \triangleq (v_1,\ldots, v_{Nm})^T$; N_p macromolecular machines $\mathbb{M} \triangleq (\mathbb{M}_1,\ldots, \mathbb{M}_{Np})$ involved in non-metabolic cellular processes such as the translation apparatus, at the concentration $M \triangleq (M_1,\ldots,M_{Np})^T$;

(ii) N_g proteins $\mathbb{P}_G \triangleq \{ \mathbb{P}_{G\,1}, \ldots, \mathbb{P}_{G\,N\,G}\}$ for which the cellular process to which the proteins belong is not specified. $P_G \triangleq (P_{G\,1}, \ldots, P_{G\,N\,G})^T$ denotes the set of concentrations of $\mathbb{P}_G$;

(iii) N_s metabolites $\mathbb{S} \triangleq (\mathbb{S}_1 ,\ldots, \mathbb{S}_{Ns})$ at the concentrations $S \triangleq (S_1 ,\ldots, S_{Ns})^T$. Among the set $\mathbb{S}$, we distinguish a subset $\mathbb{B} \triangleq (\mathbb{B}_1 ,\ldots, \mathbb{B}_{Nb})$ of metabolites which we have fixes concentrations $\bar{B} \triangleq (\bar{B}_1 ,\ldots, \bar{B}_{Nb})^T$.

P^p_{rba}: For a fixed vector of concentrations $P_G \in \mathbb{R}^{Ng}_{>0}$, and the growth rate $\mu \geq 0$; i.e., the amount of produced biomass per cell per hour,

find $Y \in \mathbb{R}^{m+p}_{\geq 0}, v \in \mathbb{R}^m$,

subject to

(C_1) $-\Omega v + \mu(C^S_Y\, Y + C^S_B\, \bar{B} + C^S_G P_G) = 0$

(C_{2a}) $\mu\,(C^M_Y\, Y + C^M_G P_G) - K_T Y \leq 0$

(C_{2b}) $-\,K'_E\, Y \leq v \leq K_E\, Y$

(C_3) $C^D_Y Y + C^D_G P_G - \bar{D} \leq 0$

where all the inequalities are component wise inequalities, $Y^T \triangleq (E^T, M^T)$ is the vector of concentrations of molecular machines and

- Ω is the stoichiometry matrix of the metabolic network of size $N_s \times N_m$, where Ω_{ij} corresponds to the stoichiometry of metabolite $\mathbb{S}_i$ in the j_{th} enzymatic reaction;

- C_Y^S (resp. C_G^S) is a $N_s \times N_y$ (resp. $N_s \times N_g$) matrix where each coefficient C_{Yij}^S corresponds to the number of metabolite $\mathbb{S}_i$ consumed (or produced) for the synthesis of one machine $\mathbb{Y}_j$ (resp. $\mathbb{P}_{Gj}$); C_{Yij}^S is then positive, negative or null if $\mathbb{S}_i$ is produced, consumed or not involved in the synthesis of one machine $\mathbb{Y}_j$ (resp. $\mathbb{P}_{Gj}$)

- C_B^S is a $N_s \times N_b$ matrix where each coefficient C_{Bij}^S corresponds to the number of metabolite $\mathbb{S}_i$ consumed (or produced) for the synthesis of one $\mathbb{B}_j$;

- K_T (K_E and K'_E, respectively) of size $N_p \times N_p$ ($N_m \times N_m$, respectively) is diagonal matrix where each coefficient $K_{T\,i}$ ($K_{E\,i}$ and $K'_{E\,i}$, respectively) is positive and corresponds to the efficiency of the molecular machine $\mathbb{M}_i$, i.e. the rate of the process per amount of the catalyzing molecular machine, (the efficiency of the enzyme $\mathbb{E}_i$, in forward and backward sense, respectively);

- C_Y^M (resp. C_G^M) is a $N_p \times N_y$ (resp. $N_p \times N_g$) matrix where each coefficient C_{Yij}^M typically corresponds to the length in amino acids of the machine $\mathbb{Y}_j$ (resp. $\mathbb{P}_{Gj}$). In some cases (for instance for the constrains on protein chaperoning), the length in amino acids can be multiplied by a coefficient, such as the fraction of the whole proteome that necessitates chaperoning;

- $\overline{D}$ is a vector size of N^c, where N^c is the number of volume and surface areas for which density constraints are considered. $\overline{D}^i$ is the density of molecular entity with respect to the volume or surface area. Densities are typically expressed as a number of amino-acid residues by volume or surface area.

- C_Y^D (resp. C_G^D) is a $N^c \times N_y$ (resp. $N^c \times N_G$) matrix where each coefficient C_{Yij}^D typically corresponds to the density of one machine $\mathbb{Y}_j$ (resp. $\mathbb{P}_{Gj}$) in the compartment i. By construction, we have one unique localization per machine.

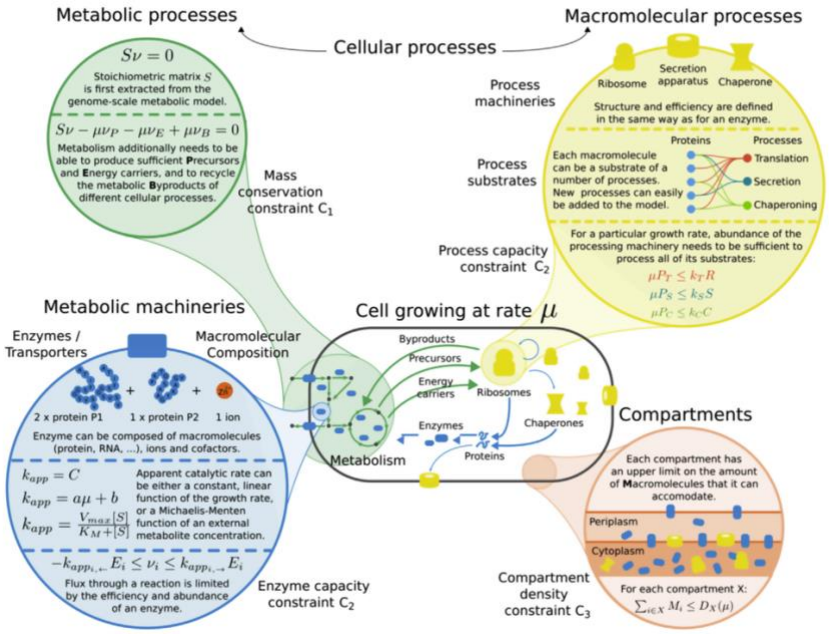

Figure 2: **A visual representation of RBA models**. Adapted from "Automated generation of bacterial resource allocation models", by Bulovíc et al., (2019), Elsevier. Copyright 2023 by RightsLink

In summary, the optimization problem finds the optimal solution, where the metabolic network can still generate all required metabolites for biomass production and keep the mass balance (C1), all molecular machinery (i.e., enzymes, transporters) have sufficient capacity to ensure the function of the cell (C2a, 2b) and the intracellular densities of the different cellular compartments and membranes stay within a predefined limit (C3).

2.5 The Crabtree Effect

S. Cerevisiae has long been categorized as a glucose-sensitive yeast strain. This means that the respiration process gets increasingly repressed with growing glucose concentration (Fiechter et al., 1992). However, it has been shown that as the glucose concentration increases the rate of aerobic fermentation increases as well. This simultaneous inhibition of respiration and augmentation of fermentation at high glucose concentrations is known as the Crabtree Effect (De Deken, 1966).

Furthermore, it has been shown that in a bioreactor the fermentation only starts to appear after a so-called critical dilution rate (which differs from strain to strain) has been reached (Van Dijken et al., 2000).

Table 1

Critical dilution rates of four *S. cerevisiae* strains. Taken from "An interlaboratory comparison of physiological and genetic properties of four Saccharomyces cerevisiae strains", by Van Dijken et al. (2000), Elsevier. Copyright 2023 by RightsLink

Strain	Critical Dilution Rate (h^{-1})
CBS 8066	0.34
BAY.17	0.32
X2180	0.22
CEN.PK122	0.27

The emergence of the Crabtree Effect is perplexing since it involves abandoning the more efficient energy generation method in respiration and opting for the less effective strategy of fermentation. Therefore, reasons for the Crabtree Effect have been researched intensively and different conclusions have been reached (Molenaar et al., 2009). One of the prevailing theories is that the Crabtree phenotype is an adaptation to the enzyme properties as rapid growth needs high enzyme mass to generate faster fluxes (Nilsson & Nielsen, 2016). Flux balance analysis on *S. cerevisiae* GEMs has not been able to demonstrate the Crabtree Effect without imposing specific constraints to induce the effect (Oftadeh et al., 2021).

3 Methods

In this section we describe how we generated our RBA model of *S. cerevisiae*, how we obtained and processed additional data and how we refined and curated our resulting model using this data.

3.1 Computational Tools and Code

3.1.1 Tools

To generate our base RBA model, we used RBApy version 2.0 which is an open-source python package[1] that can automatically create RBA models based on a GEM coded in Systems Biology Markup Language (SBML), the amino acid sequences of the organism's ribosome and chaperones as well as the nucleotide sequences of the organism's tRNA and rRNA in the FASTA format (Bulovíc et al., 2019, Hucka et al., 2003).

[1] https://github.com/SysBioInra/RBApy

RBApy represents the model through different files in eXtensible Markup Language (XML) format and by default parameterizes it with default values that Bulović et al. (2019) gathered for *E. coli*.

Additionally, we used the RBAtools software package[2] version 1.0.1, which builds on top of RBApy and provides a python programming interface for RBA models with functionalities like setting a fixed growth rate or changing certain parameter values (Bodeit et al., 2022). We used these functionalities to streamline the developing process of our model as it allowed us to efficiently test and evaluate our model.

3.1.2 iMM904RBA

Utilizing RBApy we produced a python package called iMM904RBA, which offers multiple functions to automate the generation of our resulting RBA model with no additional requirements.

It features multiple python scripts, each corresponding to a step in the model curation process outlined in Chapter 3.3. The file *model_curation.py* arranges all the different scripts and automatically creates our final curated RBA model.

The whole package can be found on GitLab[3].

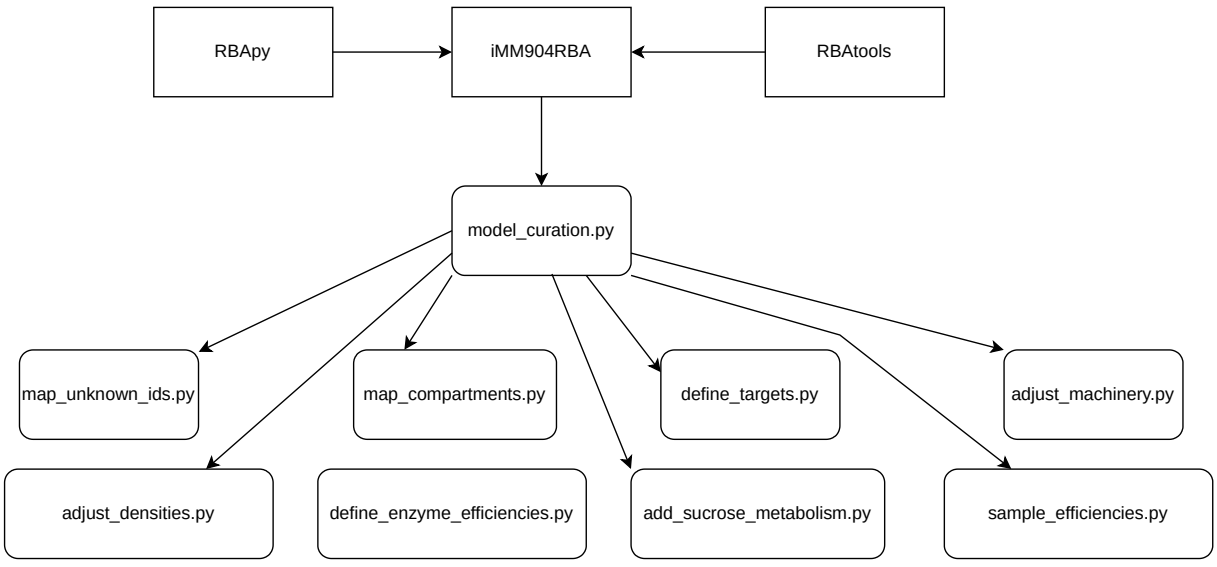

Figure 3: A visualization of the iMM904RBA package. IMM904RBA offers scripts for every part of the model curation and a script that ties all the different steps together and will generate our final model. We use the packages RBApy and RBAtools to help in the generation of our curated RBA model.

[2] https://github.com/SysBioInra/rbatools

[3]https://gitlab.cs.uni-duesseldorf.de/ccb/students/bachelor/nazarenus-resource-balance-analysis-of-saccharomyces-cerevisiae/-/tree/main/iMM904RBA

3.2 Model Generation

3.2.1 Choosing the GEM

We decided to base our RBA model on the *i*MM904 GEM of *S. cerevisiae* that is freely available at the BiGG Models database (King et al., 2016). Thanks to its well-defined naming conventions and annotations, the *i*MM904 model proved to be highly compatible with RBApy's method of generating our baseline model. This made it easier and more efficient to build and analyze the RBA model especially during the beginning of our research where we needed to tweak and regenerate the model multiple times.

We also contemplated using Yeast7 or Yeast8 respectively, as they span more genes, reactions and metabolites and would allow us to compare our simulation results more meaningfully against the ecYeast7 / ecYeast8 results. However, it became very clear to us early on that generating a solvable RBA model out of these GEMs would require much more time than with *i*MM904 due to their different naming conventions, annotations, and the greater model sizes.

Therefore, we prioritized showcasing the possibility of creating an accurate RBA model for a eukaryote like *S. cerevisiae* over the comparability to other simulation results and moved forward with *i*MM904.

Table 2

A comparison of 3 different S. cerevisiae GEMs: iMM904, Yeast7 and Yeast8.

GEM	Reactions	Metabolites	Genes
***i*MM904**	1577	1226	905
Yeast 7	3493	2218	916
Yeast 8	4063	2744	1160

3.2.2 Ribosome, Chaperone and tRNA Sequences

For RBApy to generate our first baseline RBA model of *S. cerevisiae* we needed to gather the amino acid sequences for all ribosomal proteins, chaperones, as well as the nucleotide sequences of the tRNA and rRNA in FASTA format.

In *S. cerevisiae* the ribosome consists of one small 40S subunit which contains the 18S ribosomal RNA, and the large 60S subunit, containing the 5S, 5.8S and 25S rRNAs (Woolford & Baserga, 2013).

We retrieved the nucleotide sequences in FASTA format for the 5S, 5.8S, 18S and 25S rRNA of *S. cerevisiae* from the RNA database RNAcentral (release 22) (Sweeney et al., 2019).
For the ribosomal proteins we examined the list of cytoplasmic ribosomal proteins of *S. cerevisiae* gathered by Planta and Mager (1998) and excluded any duplicates. Then, we retrieved the amino acid sequences for all 78 ribosomal proteins from the UniProt database (release 2023_01) (Bateman et al., 2022).
In their study Brownridge et al. (2013) ranked 63 different chaperones of *S. cerevisiae* for their overall folding workload based on their total substrate fluxes. We extracted the top 15 chaperones that Brownridge et al. (2013) found and again utilized the UniProt database to acquire the amino acid sequences in FASTA format for all 15 chaperones.
Finally, the nucleotide sequences of the tRNAs were downloaded from the tRNAdb (Jühling et al., 2009).

3.2.3 Generating the Baseline Model

After downloading the *i*MM904 GEM and gathering all the necessary nucleotide and amino acid sequences we were now able to utilize the script *generate_rba_model.py* from RBApy to create our first baseline RBA model based on our GEM and the information we provided.
This baseline model is mostly constrained by default values that Bulović et al. (2019) gathered for *E. coli*, and we now need to adjust the constraints and curate the different parts of the model to better match the experimental data of *S. cerevisiae*.

3.3 Model Curation

3.3.1 Mapping Metabolites and Proteins

During the initial model generation, RBApy is unable to match a few proteins, cofactors and metabolites that can be found in UniProt to their ID in the *i*MM904 GEM. To incorporate these metabolites and proteins in our model we needed to map the UniProt names to the corresponding ID in the files *metabolites.tsv* and *unknown_proteins.tsv* and then regenerate the model.

3.3.2 Mapping Different Cellular Compartments Together

By default, RBApy creates a separate cellular compartment for every subcellular location that is defined in UniProt for the given organism. Although there is no upper limit on the number of cellular compartments an RBA model can integrate, each compartment adds a lot of complexity

to the model through density constraints and target concentrations for proteins. This is one of the major pitfalls that Goelzer & Fromion (2019), discussed in their recent paper "*RBA for eukaryotic cells: foundations and theoretical developments"*. To minimize this potential defect, we reduced the total amount of compartments that are differentiated in our model from 24 to 7, by merging certain compartments together based on their cellular functions. Because of this mapping, we were able to increase the number of different cellular compartments only slightly compared to the RBA model of *E. coli*, which reduces the complexity considerably.
The detailed compartment mapping can be found in our GitLab[4].

3.3.3 Defining Metabolite and Macromolecular Targets

One of the major parts of an RBA model are metabolite and macromolecular targets. These are defined concentrations and fluxes that the model must be able to generate to consider itself in a functional state.
We added targets for certain macromolecules that act as carbon storage in the cell, as well as relevant membrane lipids, taking the stoichiometry defined in the biomass function of *i*MM904 as the target concentration. Also, we increased the default target for the methionine tRNA as it is used as the translation initiator in *S. cerevisiae* and a too low concentration would bottleneck the speed of translation and therefore hinder growth (Kapp et al., 2006).

3.3.4 Adjusting the Molecular Machinery

Another constraint that an RBA model considers are the machinery costs, which means that to be viable, the cell needs to not only produce all target components, but also the machines that assemble or break down these components.
By default, RBApy generates the translation, transcription, degradation, and folding machinery based on default values that were gathered for *E. coli* and the chaperone, ribosome and tRNA information we provided in 3.2.2.
To further improve on that, we additionally implemented the Sec61/SecY complex that is used for protein translocation between the cytosol and endoplasmatic reticulum in *S. cerevisiae* as our secretion machinery (Osborne et al., 2005).

[4]https://gitlab.cs.uni-duesseldorf.de/ccb/students/bachelor/nazarenus-resource-balance-analysis-of-saccharomyces-cerevisiae/-/blob/main/model/data/location_map.tsv

3.3.5 Sucrose Metabolism

In *S. cerevisiae* sucrose is converted extracellularly by invertase into fructose and glucose (Basso et al., 2011), however in RBA the model will not consider changes in the external metabolite concentration once they are set in the medium. This leads to our model not being able to simulate growth on sucrose. However, to showcase the flexibility of an RBA model, we adjusted the invertase reaction to convert extracellular sucrose into fructose and glucose in the cytoplasm. With this change our model is able to simulate growth on sucrose. This approach could be used for all metabolites that behave in a similar way.

3.3.6 Defining Enzyme Efficiencies

Judging from the success of the ecYeast model we expect the introduction of enzymatic constraints to be one of the biggest improvements regarding predictive accuracy when comparing RBA models to regular GEMs. Not only is RBA considering the additional mass and construction costs of the enzymes, but it also takes the catalyzing efficiency of each enzyme for every reaction into account. By default, our RBA model uses one constant efficiency for all transporter enzymes and one constant efficiency for all other enzymes.

To start, we adopted the non-transporter and transporter enzyme efficiencies from the RBA model of *E. coli* (Bulović et al., 2019).

To further improve on that, we established a distinct enzyme efficiency for amino acid transport. This enables us to have more granular control and to portray more complex phenomena, such as the alteration of amino acid transport rate on different carbon sources in *S. cerevisiae* (Peter et al., 2006).

Additionally, to improve the modelling of the uptake rate of external metabolites we implemented Michaelis-Menten kinetics for all external transporter enzymes based on the external metabolite concentration defined in the medium.

3.3.7 Density Constraints

Another major part of an RBA model are the maximal macromolecular density constraints for each compartment, as they govern much of the necessary resource allocation that is being computed. To find a good match for the densities in our model, we used the data from Ho et al. (2018) who unified the protein abundance measurements for *S. cerevisiae* of 21 studies to represent protein molecules per cell.

In order to curate our model, we need to calculate both the percentage of enzymatic and non-enzymatic proteins that each compartment holds (in millimoles of amino acid residues per gram of cell dry weight [mmol.AA/gCDW]).

To obtain this data we took the heuristic that all proteins present in our model should be classified as enzymatic proteins and all proteins that are not present in our model but have been measured in the 21 different studies from Ho et al. (2018) should be classified as non-enzymatic.

We calculated the mmol.AA/gCDW of each protein measurement, mapped each protein to their corresponding compartment and then calculated both the percentage of enzymatic proteins per compartment and the percentage of non-enzymatic proteins per compartment for each of the 21 different studies, as well as the median and the mean value of all studies.

We then ran simulations for aerobic growth on minimal, minimal with amino acids, and complex glucose media for our model using each of our resulting densities, comparing the average relative error between each of the density iterations and saw that the data from Nagaraj et al. (2012) led to the best results with an overall mean relative error of 8,4% across the three media (Figure 4). Therefore, we settled on the densities resulting from the protein data of Nagaraj et al. (2012) for our final model.

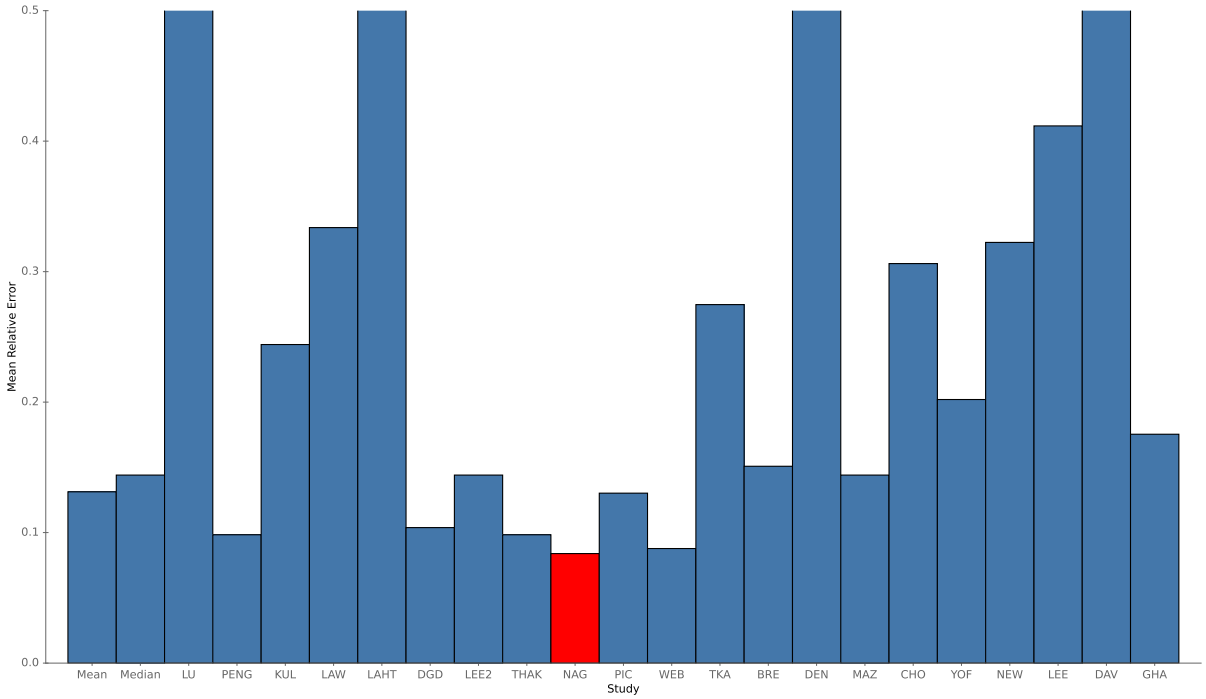

Figure 4: Density constraints. A comparison of the mean relative error from growth simulations on minimal, minimal with amino acids and complex glucose media where the model is using the densities calculated from the protein measurements of each study, as well as the mean and median values across all studies. The lowest mean relative error was found using the densities derived from the protein measurements of Nagaraj et al. (2012) (shown in red). The mapping of abbreviations to the respective study can be found in the paper "Unification of Protein Abundance Datasets Yields a Quantitative Saccharomyces cerevisiae Proteome" from Ho et al. (2018).

3.3.8 Sampling Non-Transporter Enzyme Efficiencies

To improve on the non-transporter enzyme efficiencies, we decided to sample 100 random multiplicative factors from a standard normal distribution for every non-transporter enzyme efficiency and compare the outcomes of growth simulations using these efficiencies on minimal, minimal with amino acids, and complex glucose media to the experimental data. We also did growth simulations using the enzyme efficiency which Bulović et al. (2019) used in their *E. coli* RBA model and using the enzyme efficiencies aggregated from BRENDA that are used in the ecYeast7 model by Sánchez et al (2017) (Figure 5).

We found the lowest mean relative error to be in one of our samples with 6.83% and used the corresponding efficiencies in our final model.

The complete list of all non-transporter enzyme efficiencies can be found in GitLab[5].

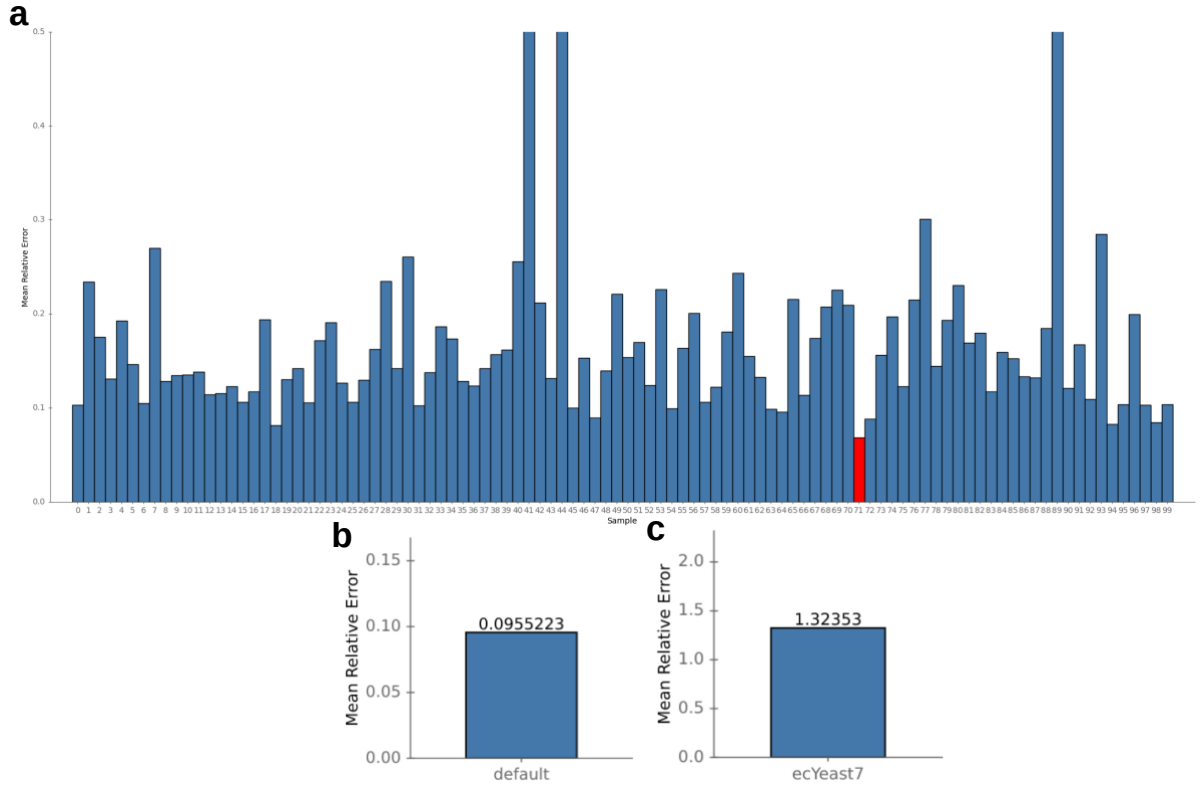

Figure 5: Enzyme Efficiency Sampling. A comparison of the mean relative error from growth simulations on minimal, minimal with amino acids, and complex glucose media where the model is using (a) randomized enzyme efficiencies, (b) the default enzyme efficiency and (c) the enzyme efficiencies that were used in the ecYeast7 model from Sánchez et al. (2017). Sample 71 (shown in red) led to the lowest relative error over the three media.

[5]https://gitlab.cs.uni-duesseldorf.de/ccb/students/bachelor/nazarenus-resource-balance-analysis-of-saccharomyces-cerevisiae/-/blob/main/iMM904RBA/data/sampledEfficiencies.xlsx

4 Results

4.1 Growth Simulations Under Different Carbon Sources

Paralleling the simulations done by Sánchez et al. (2017) we simulated aerobic, non-restrictive growth on 11 different carbon sources in 3 different media and compared the results with experimental data from Tyson et al. (1979) and Van Dijken et al. (2000) (Figure 6).

Using our curated RBA model, we managed to achieve a pretty good fit to the experimental results with an average absolute error of 0.079 and a mean relative error of 32%.

In order to assess the efficacy of each step of our model curation process, we carried the same growth simulations out following each stage and compared the average relative error (Figure 7).

We can see, that by increasing the methionine tRNA target as well as defining targets for specific macromolecules we managed to induce growth in our simulations.

Another major improvement came from introducing Michaelis-Menten kinetics for the external transporters as well as a distinct amino-acid intake efficiency which made the model much more accurate.

Finally, the calculation of density constraints based on the experimental protein abundance data from *Nagaraj et al. (2012)* brings our simulation results to a comparable level to those of the ecYeast models (Figure 1).

Overall, with minimal manual curation, we achieve slightly worse results than the highly curated ecYeast7 or ecYeast8 models. Nevertheless, the simulation results make clear that the RBA method can achieve a lot more accurate growth rate predictions than FBA on a typical GEM and shows promise for further efforts in RBA modelling of *S. cerevisiae* and eukaryotes in general.

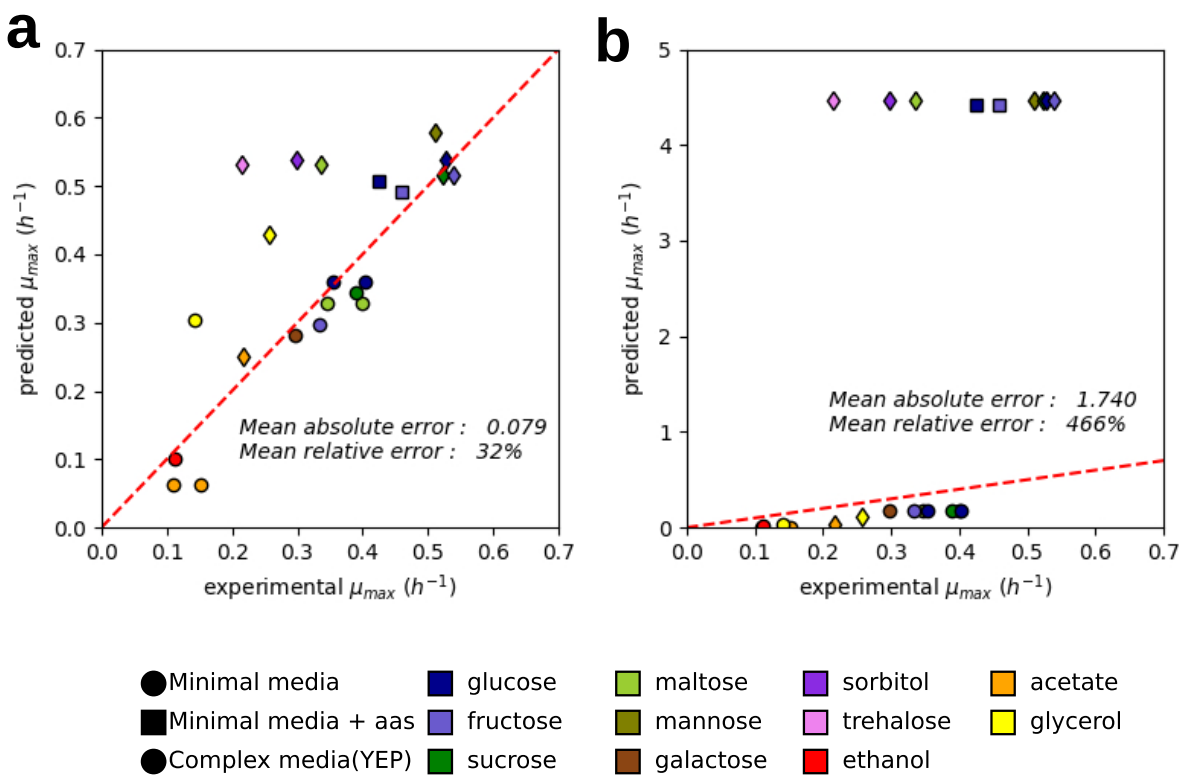

Figure 6: Comparison of Growth Simulations using RBA and FBA. Results of aerobic growth simulations using 11 different carbon sources in minimal, minimal with amino acids and complex media. We can see improved predictive accuracy in our final RBA model of S. cerevisiae (a) when compared to using standard FBA on the iMM904 GEM (b).

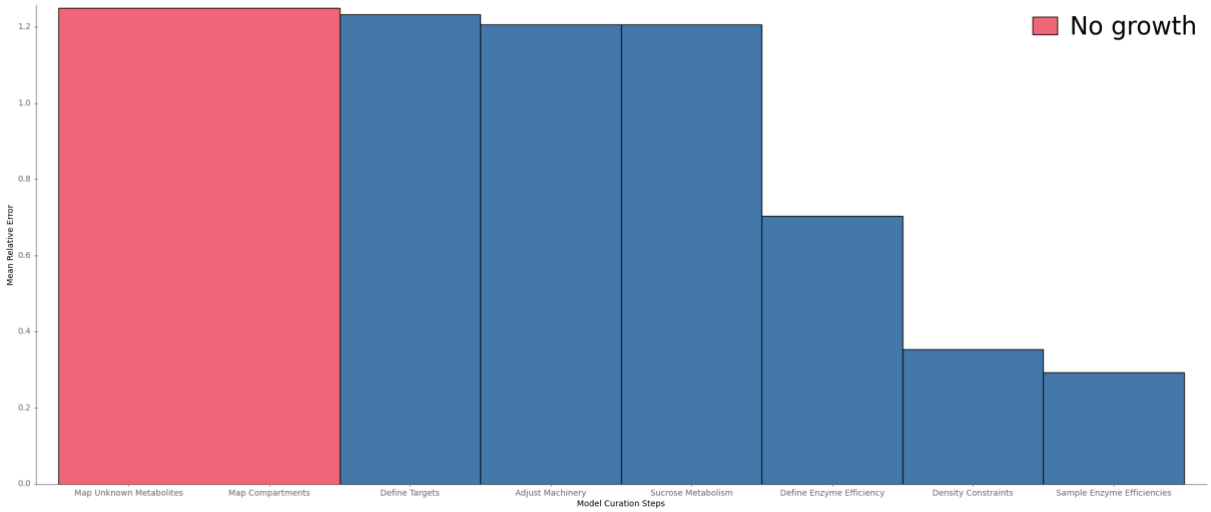

Figure 7: Effectiveness of the model curation. Mean relative error of aerobic growth simulations using 11 different carbon sources in minimal, minimal with amino acids and complex media for every step of the model curation process. We can see big improvements at the introduction points of targets, enzyme efficiencies and density constraints.

4.2 Protein Allocation

In their recent study Lahtvee et al. (2017) have grown *S. cerevisiae* under chemostat conditions at a growth rate of $0.1\ h^{-1}$ and quantified the protein and mRNA abundances. Using the KEGG database (release 106) we categorized each protein into their most common metabolic pathway (Kanehisa et al., 2000). To investigate in how far the allocation of enzymes in our model matches the experimental data we compared the percentage of protein mass per metabolic pathway between the data from Lahtvee et al. (2017) and the results of our growth simulations (Figure 8).

We were able to see that the biggest relative mismatch in terms of protein allocation in our model and the data from Lahtvee et al. (2017), seems to be the translation as well as the folding, sorting and degradation pathways. This suggests that potential areas to enhance our model further could be the translation, folding, and degradation machineries that we left mostly untouched in our model curation.

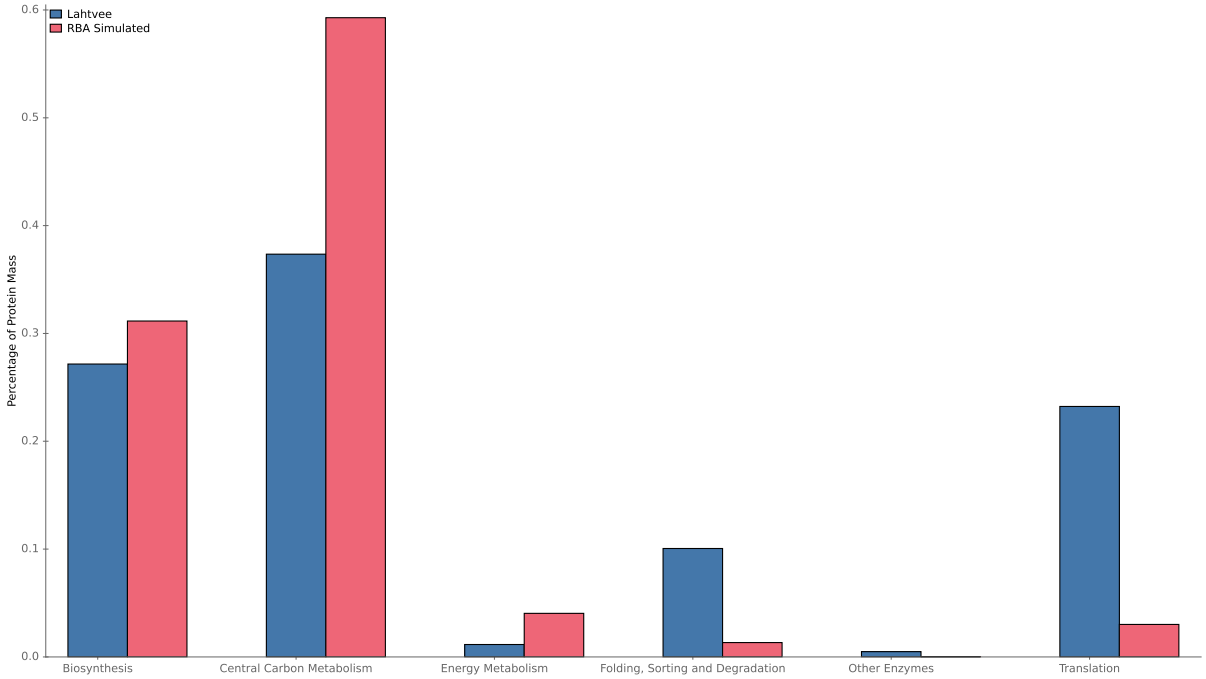

Figure 8: Comparison of protein allocation. A comparison of the percentage of protein mass per metabolic pathway that was simulated using our curated RBA model and experimental data from Lahtvee et al. (2017). In our model most of the proteins are allocated to the biosynthesis and central carbon metabolism pathways.

4.3 The Crabtree Effect

As our model is constrained by the total enzyme mass, we tested whether we could observe the shift in metabolic function known as the Crabtree Effect which would support the theory by Nilsson and Nielsen (2016) that the Crabtree Effect is an adaptation to the limitation of enzyme mass. As we ran the simulations, we identified that we could both see the onset of ethanol

production at increasing glucose concentrations as well as spot a critical dilution rate (CDR) of 0.12 h^{-1} where fermentation starts to begin (Figure 9).

Therefore, without imposing specific constraints on our model, we can observe the emergence of the Crabtree Effect.

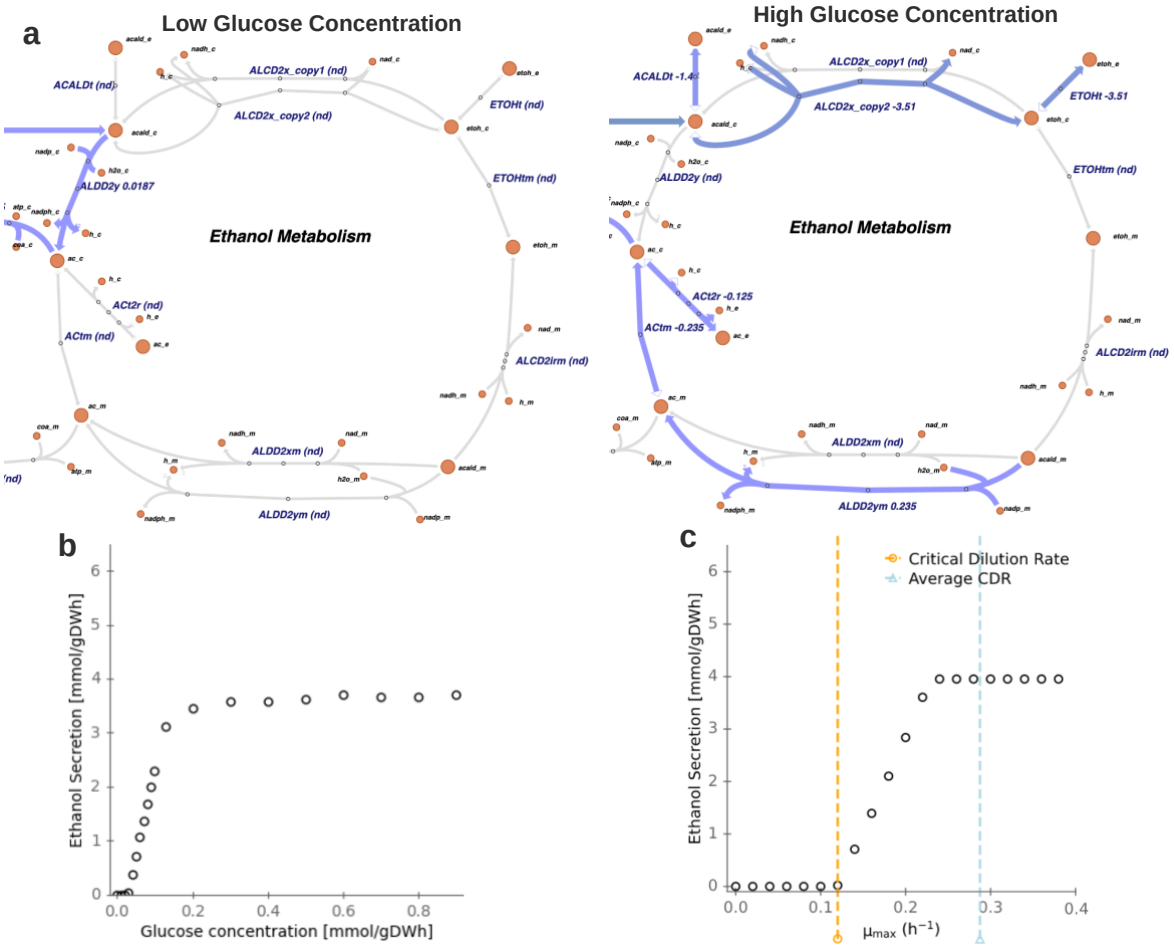

Figure 9: The Crabtree Effect. We show flux maps (a) where reaction fluxes are colored blue. We can observe increasing fluxes in the ethanol metabolism as well as ethanol secretion (shown in red) at higher glucose concentrations. We see the onset of ethanol secretion and the fermentation process as glucose concentration increases (b). We also measure a critical dilution rate of 0.12 h^{-1} (c).

4.4 Optimal Flux Simulation

Parsimonious Flux Balance Analysis (pFBA) is a variant of FBA, which seeks to minimize the sum of fluxes in the model while maintaining optimum flux through the objective function. In essence, this approach identifies the least biologically "expensive" usage of an organism's metabolism to achieve high growth rates (Jenior et al., 2020).

We compared the resulting fluxes of our model when simulating growth on a complex glucose medium against the resulting fluxes of pFBA simulations on a similar medium and saw that both methods share more than half of their reactions (Figure 10b). The overlap makes sense, as

both methods try to identify the best usage of the organism's metabolism. Additionally, we saw that RBA computes a lot more flux in total (Figure 10a), which can be attributed to the different targets that we set in our model and could explain the lower and more accurate resulting growth rates we get when using RBA.

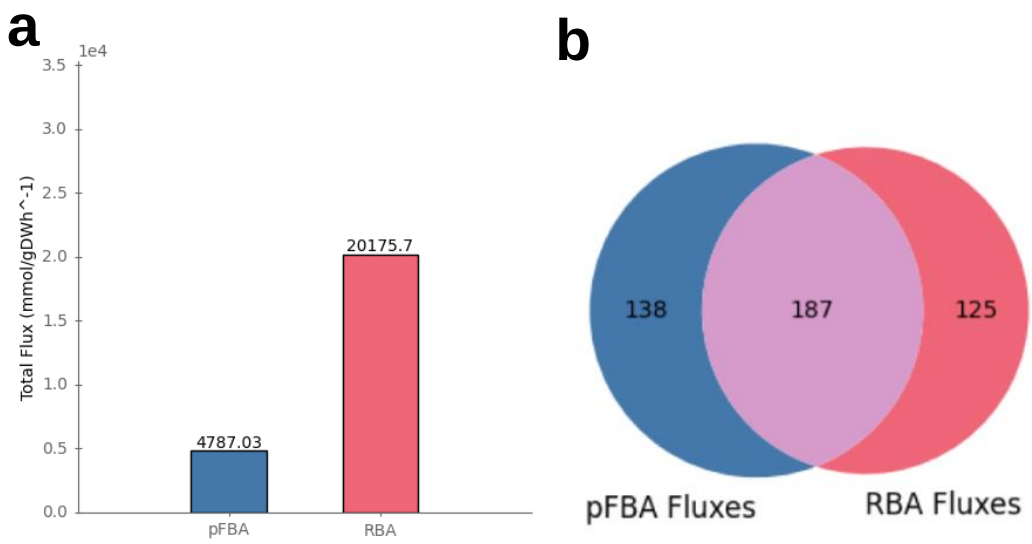

Figure 10: Flux Simulation. A comparison of (a) total flux when simulating growth on complex glucose medium with pFBA and our curated RBA model and (b) shared number of reaction fluxes in both methods.

5 Discussion

5.1 Evaluation of our Results

We have created an RBA model for *S. cerevisiae* that is able to accurately predict aerobic growth rates on different carbon sources, as well as specific metabolic phenomena like the Crabtree Effect. The results of our simulations give us confidence that modelling of eukaryotes via RBA is a feasible way to improve predictive accuracy of a GEM.

We can see from our analysis in Figure 7, that the biggest factors in our model curation process were the introduction of target concentrations found in the biomass function of *i*MM904, defining enzyme efficiencies and the calculation of density constraints based on measured protein data.

As we left most of the process machinery untouched with the values Bulović et al. (2019) gathered for *E. coli* and only adjusted parts of the folding and secretion machinery, we see only little improvement when applying this step. This also seems to be represented in the results of

our protein allocation comparison (Figure 8), where our model severely underrepresents the amount of protein that is needed for the translation, folding, sorting and degradation processes. The emergence of the Crabtree Effect shows the potency of the implementation of enzyme limitations. However, our results are not entirely accurate when compared to the experimental data, as we show a much lower critical dilution rate of 0.12 when compared to the data of Van Dijken et al. (2000) (Figure 9c). This indicates to us that the enzyme efficiencies we applied also still have room for improvement, especially when it comes to the transporter enzymes and our use of Michaelis-Menten kinetics.

Nevertheless, it shows great promise for the RBA modelling method that our model can portray a key phenotypic behavior of *S. cerevisiae* like the Crabtree Effect without the necessity of imposing specific constraints.

When comparing our results against the results of other modelling methods like GECKO and the resulting *ecYeast* GEMs, we can see that we slightly underperform in some areas, as they average a lower relative error on the same growth simulations and a similar relative error across a multitude of different media (Figure 1) as well as being capable of producing the Crabtree Effect (Sánchez et al., 2017).

However, we still see a lot of potential in our model and the RBA framework, as it is very flexible and could incorporate a lot more details and processes than we were able to integrate in the rather short time span of this thesis. Which could mean that with some further refinement the GECKO results could be matched or even surpassed.

Therefore, we believe that our model provides a good starting point for further improvements in the future.

5.2 Further Improvements

As previously discussed, one major area that can be improved in our model are the molecular machineries for the translation, folding and degradation processes. To improve on those, we would need to investigate in how far those processes differ in *S. cerevisiae* when compared to *E. coli* and adjust the representation in our model accordingly.

Furthermore, adjusting the Michaelis-Menten kinetics that we set for all external transporter enzymes could lead to improvements when it comes to phenomena that rely on accurate representation of the intake rate of external metabolites.

Finally, improving on the enzyme efficiencies that we arrived on through random sampling (Figure 5) by integrating accurate experimental measurements of enzyme kinetic data could lead to further improvements of our model.

6 Conclusion

This thesis presented a way to utilize Resource Balance Analysis to create an accurate model of the organism *S. cerevisiae.* We have also created a python package that can be used to either generate our final model or used as a toolbox to adjust certain parts of an RBA model.

We compared our results to another modelling approach that incorporates enzyme constraints into a GEM and have found that our approach can lead to similar results in terms of growth simulation. Additionally, we were also able to see a key metabolic phenomenon in form of the Crabtree Effect arise in our model.

We have shown that creating RBA models for eukaryotes such as *S. cerevisiae* can lead to improved predictive accuracy when compared to a standard GEM, even with minimal required experimental data and believe that our model can be used as a baseline for further RBA modelling of *S. cerevisiae.*

References

Sánchez, B. M., Zhang, C., Nilsson, A., Lahtvee, P., Kerkhoven, E. J., & Nielsen, J. (2017). Improving the phenotype predictions of a yeast genome-scale metabolic model by incorporating enzymatic constraints. *Molecular Systems Biology*, *13*(8), 935. https://doi.org/10.15252/msb.20167411

Orth, J. D., Thiele, I., & Palsson, B. O. (2010). What is flux balance analysis? *Nature Biotechnology*, *28*(3), 245–248. https://doi.org/10.1038/nbt.1614

Botstein D, Chervitz SA, Cherry JM. Yeast as a model organism. Science. 1997 Aug 29;277(5330):1259-60. doi: 10.1126/science.277.5330.1259. PMID: 9297238; PMCID: PMC3039837.

Mo ML, Palsson BO, Herrgård MJ. Connecting extracellular metabolomic measurements to intracellular flux states in yeast. BMC Syst Biol. 2009 Mar 25;3:37. doi: 10.1186/1752-0509-3-37. PMID: 19321003; PMCID: PMC2679711.

Bateman, A., Martin, M., Orchard, S., Magrane, M., Ahmad, S., Alpi, E., Bowler-Barnett, E. H., Britto, R., Bye-A-Jee, H., Cukura, A., Denny, P., Dogan, T., Ebenezer, T., Fan, J., Garmiri, P., Da Costa Gonzales, L. J., Hatton-Ellis, E., Hussein, A., Ignatchenko, A., . . . Zhang, J. (2022). UniProt: the Universal Protein Knowledgebase in 2023. *Nucleic Acids Research*, *51*(D1), D523–D531. https://doi.org/10.1093/nar/gkac1052

Karthik Raman, Nagasuma Chandra, Flux balance analysis of biological systems: applications and challenges, *Briefings in Bioinformatics*, Volume 10, Issue 4, July 2009, Pages 435–449, https://doi.org/10.1093/bib/bbp011

Lu, H., Li, F., Sánchez, B.J. et al. A consensus S. cerevisiae metabolic model Yeast8 and its ecosystem for comprehensively probing cellular metabolism. Nat Commun 10, 3586 (2019). https://doi.org/10.1038/s41467-019-11581-3

Aung HW, Henry SA, Walker LP (2013) Revising the representation of fatty acid, glycerolipid, and glycerophospholipid metabolism in the consensus model of yeast metabolism. ***Ind Biotechnol* 9**: 215–228

Bulović, A., Fischer, S., Dinh, M., Golib, F., Liebermeister, W., Poirier, C., Tournier, L., Klipp, E., Fromion, V., & Goelzer, A. (2019). Automated generation of bacterial

resource allocation models. *Metabolic Engineering*, *55*, 12–22. https://doi.org/10.1016/j.ymben.2019.06.001

King ZA, Lu JS, Dräger A, Miller PC, Federowicz S, Lerman JA, Ebrahim A, Palsson BO, and Lewis NE. **BiGG Models: A platform for integrating, standardizing, and sharing genome-scale models** (2016) Nucleic Acids Research 44(D1):D515-D522. doi:10.1093/nar/gkv1049

Coppens, L., Tschirhart, T., Leary, D.H., Colston, S.M., Compton, J.R., Hervey, W.J., IV, Dana, K.L., Vora, G.J., Bordel, S. and Ledesma-Amaro, R. (2023), Vibrio natriegens genome-scale modeling reveals insights into halophilic adaptations and resource allocation. Mol Syst Biol e10523. https://doi.org/10.15252/msb.202110523

Kapp LD, Kolitz SE, Lorsch JR. Yeast initiator tRNA identity elements cooperate to influence multiple steps of translation initiation. RNA. 2006 May;12(5):751-64. doi: 10.1261/rna.2263906. Epub 2006 Mar 24. PMID: 16565414; PMCID: PMC1440903.

Ho, B., Baryshnikova, A. & Brown, G. E. (2018). Unification of Protein Abundance Datasets Yields a Quantitative Saccharomyces cerevisiae Proteome. *Cell systems*, *6*(2), 192-205.e3. https://doi.org/10.1016/j.cels.2017.12.004

Chang, A., Jeske, L., Ulbrich, S., Hofmann, J., Koblitz, J., Schomburg, I., Neumann-Schaal, M., Jahn, D., & Schomburg, D. (2021). BRENDA, the ELIXIR core data resource in 2021: new developments and updates. *Nucleic Acids Research*, *49*(D1), D498–D508. https://doi.org/10.1093/nar/gkaa1025

Goelzer, A., & Fromion, V. (2017). Resource allocation in living organisms. *Biochemical Society Transactions*, *45*(4), 945–952. https://doi.org/10.1042/bst20160436

Goelzer, A., & Fromion, V. (2019). RBA for eukaryotic cells: foundations and theoretical developments. *BioRxiv (Cold Spring Harbor Laboratory)*. https://doi.org/10.1101/750182

Fiechter, A., Fuhrmann, G., & Käppeli, O. (1992). Regulation of Glucose Metabolism in Growing Yeast Cells. *Advances in Microbial Physiology*, 123–183. https://doi.org/10.1016/s0065-2911(08)60327-6

Van Dijken, J., Bauer, J. M., Brambilla, L., Duboc, P., François, J. M., Gancedo, C., Giuseppin, M. L. F., Heijnen, J. J., Hoare, M., Lange, H., Madden, E., Niederberger, P., Nielsen, J., Parrou, J. L., Petit, T., Porro, D., Reuss, M., Van Riel, N., Rizzi, M., . . . Pronk, J. T. (2000). An interlaboratory comparison of physiological and genetic properties of four Saccharomyces cerevisiae strains. *Enzyme and Microbial Technology*, *26*(9–10), 706–714. https://doi.org/10.1016/s0141-0229(00)00162-9

Molenaar, D., Van Berlo, R. J. P., De Ridder, D., & Teusink, B. (2009). Shifts in growth strategies reflect tradeoffs in cellular economics. *Molecular Systems Biology*, *5*(1), 323. https://doi.org/10.1038/msb.2009.82

Nilsson, A., & Nielsen, J. (2016). Metabolic Trade-offs in Yeast are Caused by F1F0-ATP synthase. *Scientific Reports*, *6*(1). https://doi.org/10.1038/srep22264

Lahtvee, P., Sánchez, B. M., Smialowska, A., Kasvandik, S., Elsemman, I. E., Gatto, F., & Nielsen, J. (2017). Absolute Quantification of Protein and mRNA Abundances Demonstrate Variability in Gene-Specific Translation Efficiency in Yeast. *Cell Systems*, *4*(5), 495-504.e5. https://doi.org/10.1016/j.cels.2017.03.003

Jenior, M. L., Moutinho, T. J., Dougherty, B. V., & Papin, J. A. (2020). Transcriptome-guided parsimonious flux analysis improves predictions with metabolic networks in complex environments. *PLOS Computational Biology*, *16*(4), e1007099. https://doi.org/10.1371/journal.pcbi.1007099

Bordbar, A., Monk, J. M., King, Z. A., & Palsson, B. O. (2014). Constraint-based models predict metabolic and associated cellular functions. *Nature Reviews Genetics*, *15*(2), 107–120. https://doi.org/10.1038/nrg3643

De Deken, R. H. (1966). The Crabtree Effect: A Regulatory System in Yeast. *Journal of General Microbiology*, *44*(2), 149–156. https://doi.org/10.1099/00221287-44-2-149

Bertsimas, D., & Tsitsiklis, J. N. (1997). *Introduction to Linear Optimization*.

GLPK - GNU Project - Free Software Foundation (FSF). (n.d.). https://www.gnu.org/software/glpk/

Ilog CPLEX 8.0: User's Manual. (2002).

Bodeit, O., Samir, I. B., Karr, J. R., Goelzer, A., & Liebermeister, W. (2022). RBAtools: a programming interface for Resource Balance Analysis modelling. *BioRxiv (Cold Spring Harbor Laboratory)*. https://doi.org/10.1101/2022.12.19.521060

Hucka, M., Finney, A., Sauro, H. M., Bolouri, H., Doyle, J. G., Kitano, H., Arkin, A. P., Bornstein, B., Bray, D., Cornish-Bowden, A., Cuellar, A., Dronov, S., Gilles, E. D., Ginkel, M., Gor, V., Goryanin, I., Hedley, W. J., Hodgman, T. C., Hofmeyr, J., . . . Wang, J. (2003). The systems biology markup language (SBML): a medium for representation and exchange of biochemical network models. *Bioinformatics*, *19*(4), 524–531. https://doi.org/10.1093/bioinformatics/btg015

Peter, G., Düring, L., & Ahmed, A. U. (2006). Carbon Catabolite Repression Regulates Amino Acid Permeases in Saccharomyces cerevisiae via the TOR Signaling Pathway. *Journal of Biological Chemistry*, *281*(9), 5546–5552. https://doi.org/10.1074/jbc.m513842200

Hayer-Hartl, M., Bracher, A., & Hartl, F. U. (2016). The GroEL–GroES Chaperonin Machine: A Nano-Cage for Protein Folding. *Trends in Biochemical Sciences*, *41*(1), 62–76. https://doi.org/10.1016/j.tibs.2015.07.009

Brownridge, P., Lawless, C., Payapilly, A., Lanthaler, K., Holman, S. W., Harman, V. M., Grant, C. V., Beynon, R. J., & Hubbard, S. J. (2013). Quantitative analysis of chaperone network throughput in budding yeast. *Proteomics*, *13*(8), 1276–1291. https://doi.org/10.1002/pmic.201200412

Osborne, A., Rapoport, T. A., & Van Den Berg, B. (2005). PROTEIN TRANSLOCATION BY THE SEC61/SECY CHANNEL. *Annual Review of Cell and Developmental Biology*, *21*(1), 529–550. https://doi.org/10.1146/annurev.cellbio.21.012704.133214

Brownridge, P., Lawless, C., Payapilly, A., Lanthaler, K., Holman, S. W., Harman, V. M., Grant, C. V., Beynon, R. J., & Hubbard, S. J. (2013b). Quantitative analysis of chaperone network throughput in budding yeast. *Proteomics*, *13*(8), 1276–1291. https://doi.org/10.1002/pmic.201200412

Woolford, J. L., & Baserga, S. J. (2013b). Ribosome Biogenesis in the Yeast *Saccharomyces cerevisiae*. *Genetics*, *195*(3), 643–681. https://doi.org/10.1534/genetics.113.153197

Sweeney, B. A., Petrov, A. S., Burkov, B., Finn, R., Bateman, A., Szymanski, M. P., Karlowski, W. M., Gorodkin, J., Seemann, S. E., Cannone, J. J., Gutell, R. R., Fey, P., Basu, S., Kay, S., Cochrane, G., Billis, K., Emmert, D., Marygold, S. J., Huntley, R. P., . . . Williams, K. P. (2019). RNAcentral: a hub of information for non-coding RNA sequences. *Nucleic Acids Research*, *47*(D1), D221–D229. https://doi.org/10.1093/nar/gky1034

Planta, R. J., & Mager, W. H. (1998). The list of cytoplasmic ribosomal proteins of Saccharomyces cerevisiae. *Yeast*, *14*(5), 471–477. https://doi.org/10.1002/(sici)1097-0061(19980330)14:5

Nagaraj, N., Kulak, N. A., Cox, J., Neuhauser, N., Mayr, K., Hoerning, O., Vorm, O., & Mann, M. (2012). System-wide Perturbation Analysis with Nearly Complete Coverage of the Yeast Proteome by Single-shot Ultra HPLC Runs on a Bench Top Orbitrap. *Molecular & Cellular Proteomics*, *11*(3), M111.013722. https://doi.org/10.1074/mcp.m111.013722

Basso, T. O., De Kok, S., Dário, M. G., Espirito-Santo, J. C. a. D., Muller, G. V., Schlölg, P. S., Silva, C. A., Tonso, A., Daran, J., Gombert, A., Van Maris, A. J. A., Pronk, J. T., & Stambuk, B. U. (2011). Engineering topology and kinetics of sucrose metabolism in Saccharomyces cerevisiae for improved ethanol yield. *Metabolic Engineering*, *13*(6), 694–703. https://doi.org/10.1016/j.ymben.2011.09.005

Kanehisa, M. (2000). KEGG: Kyoto Encyclopedia of Genes and Genomes. *Nucleic Acids Research*, *28*(1), 27–30. https://doi.org/10.1093/nar/28.1.27

Oftadeh, O., Salvy, P., Masid, M., Curvat, M., Miskovic, L., & Hatzimanikatis, V. (2021). A genome-scale metabolic model of Saccharomyces cerevisiae that integrates expression constraints and reaction thermodynamics. *Nature Communications*, *12*(1). https://doi.org/10.1038/s41467-021-25158-6

Tyson, C. B., Lord, P. G., & Wheals, A. E. (1979b). Dependency of size of Saccharomyces cerevisiae cells on growth rate. *Journal of Bacteriology*, *138*(1), 92–98. https://doi.org/10.1128/jb.138.1.92-98.1979

List of Figures

List of Tables